Distinct kinetics of synaptic structural plasticity, memory formation, and memory decay in massed and spaced learning

Wajeeha Aziz[a,b], Wen Wang[a,c], Sebnem Kesaf[a,b,d], Alsayed Abdelhamid Mohamed[a,e], Yugo Fukazawa[a,b,f,1,2], and Ryuichi Shigemoto[a,b,d,2]

[a]Division of Cerebral Structure, National Institute for Physiological Sciences, Okazaki 444-8787, Japan; [b]Department of Physiological Sciences, The Graduate University for Advanced Studies (Sokendai), Okazaki 444-8787, Japan; [c]Department of Anatomy, Histology and Embryology, K. K. Leung Brain Research Centre, Fourth Military Medical University, Xi'an 710032, China; [d]Institute of Science and Technology Austria, Klosterneuburg 3400, Austria; [e]Department of Anatomy and Embryology, Faculty of Veterinary Medicine, South Valley University, 83523 Qena, Egypt; and [f]Core Research for Evolutional Science and Technology, Tokyo 102-0075, Japan

Edited by Richard L. Huganir, The Johns Hopkins University School of Medicine, Baltimore, MD, and approved November 7, 2013 (received for review February 20, 2013)

Long-lasting memories are formed when the stimulus is temporally distributed (spacing effect). However, the synaptic mechanisms underlying this robust phenomenon and the precise time course of the synaptic modifications that occur during learning remain unclear. Here we examined the adaptation of horizontal optokinetic response in mice that underwent 1 h of massed and spaced training at varying intervals. Despite similar acquisition by all training protocols, 1 h of spacing produced the highest memory retention at 24 h, which lasted for 1 mo. The distinct kinetics of memory are strongly correlated with the reduction of floccular parallel fiber–Purkinje cell synapses but not with AMPA receptor (AMPAR) number and synapse size. After the spaced training, we observed 25%, 23%, and 12% reduction in AMPAR density, synapse size, and synapse number, respectively. Four hours after the spaced training, half of the synapses and Purkinje cell spines had been eliminated, whereas AMPAR density and synapse size were recovered in remaining synapses. Surprisingly, massed training also produced long-term memory and halving of synapses; however, this occurred slowly over days, and the memory lasted for only 1 wk. This distinct kinetics of structural plasticity may serve as a basis for unique temporal profiles in the formation and decay of memory with or without intervals.

cerebellar motor learning | AMPA receptor reduction | synapse shrinkage and elimination

During learning, memories are formed in a specific population of neuronal circuits and are consolidated for persistence (1, 2). These memory processes are supported by discrete subcellular events such as reversible modifications in the efficacy of synaptic transmission (3–5) or persistent structural modifications in the size and number of synaptic connections (6–8). However, how these synaptic modifications relate to the dynamics of formation and decay of memories in behaving animals remains elusive. Memory formation and its persistence are also sensitive to the temporal features of stimulus presentation, as observed in the well-known "spacing effect." Training trials that include resting intervals between them (spaced training) produce stronger and longer-lasting memories than do the same number of trials with no intervals (massed training) (9). The spacing effect has been observed in a variety of explicit and implicit memory tasks (10–13), and the molecular mechanisms supporting this phenomenon have been reported (14–18). Various intracellular signaling molecules such as CREB (19), mitogen-activated protein (MAP) kinase (20, 21), and PKA (22, 23) underlie the spacing effect and are implicated in the remodeling of neuronal structures (23). In vitro studies showed that spaced stimuli induced the protrusion of new filopodia (20) and the recruitment of new synapses (24) in hippocampal neurons. However, despite the existence of numerous behavioral and molecular studies, no conjoint study has elucidated the synaptic correlates that underpin the expression of the spacing effect during learning. Here we studied the temporal evolution and decay of memory and its correlation with synaptic modifications during learning with distinct temporal patterns of training.

We used an adaptation of the horizontal optokinetic response (HOKR), which is a simple model of cerebellum-dependent motor learning. It is a compensatory eye movement for stabilization of the visual image on the retina during horizontal motion of the surroundings. A surrounding that oscillates horizontally at a given frequency causes retinal slips in naive animals and facilitates HOKR 1 h after training (HOKR adaptation) (25–27). The amount of adaptation can be quantitatively monitored, and the flocculus (Fl), which is a phylogenetically preserved cerebellar lobule, is involved in the adaptation of the HOKR (28, 29). These features render this paradigm as an experimental model, useful for investigating neural correlates and mechanisms involved in motor learning. In a previous study, we showed that the short-term adaptation of HOKR induced by 1-h training was accompanied by a rapid and transient reduction (28%) in the

Significance

Learning with resting intervals induces longer-lasting memories. However, how structural alterations in neuronal synapses correlate with temporal regulation in learning with or without intervals remain unclear. We used a cerebellar motor learning paradigm in mice using massed or spaced training. Just after the training, we found similar acquisition and AMPA-type glutamate receptor reduction in parallel fiber–Purkinje cell synapses by both protocols. However, spacing induced quicker structural modifications with halving of the synapses and spines within 4 h, thus resulting in persistent long-term memory. We demonstrate the quick development of the synaptic plasticity as a structural basis for spacing effect.

Author contributions: W.A., Y.F., and R.S. designed research; W.A., S.K., and A.A.M. performed research; W.W. contributed new reagents/analytic tools; W.W. set up the horizontal optokinetic response recording system; W.A., S.K., and Y.F. analyzed data; and W.A., Y.F., and R.S. wrote the paper.

The authors declare no conflict of interest.

This article is a PNAS Direct Submission.

Freely available online through the PNAS open access option.

[1]Present address: Department of Anatomy and Molecular Cell Biology, Graduate School of Medicine, Nagoya University, Nagoya 466-8550, Japan.

[2]To whom correspondence may be addressed. E-mail: yugo@med.nagoya-u.ac.jp or ryuichi.shigemoto@ist.ac.at.

This article contains supporting information online at www.pnas.org/lookup/suppl/doi:10.1073/pnas.1303317110/-/DCSupplemental.

number of AMPA receptors (AMPARs) in parallel fiber (PF) to Purkinje cell (PC) synapses, whereas the long-term adaptation induced by repeated 1-h training over 5 d was accompanied by a slowly developing reduction (45%) of PF–PC synapses (30). Despite recent controversies on the role of long-term depression (LTD) and a postulated role of long-term potentiation in cerebellar motor learning (31–33), this study first showed that LTD as a form of reduced AMPARs in PF–PC synapses does occur in physiological learning.

In the present study, we further examined how the spacing effect is correlated with the structural plasticity in PF–PC synapses. We showed that spaced training including 1-h intervals induced stable long-lasting memories within 4 h after the training, which was accompanied by a rapid and long-lasting (>1 mo) reduction of PF–PC synapses after a transient reduction in AMPAR density and shrinkage of PF–PC synapses and PC spines. One hour of massed training also induced a gradual reduction of the PF–PC synapses, which reached the same level as that observed for the spaced training 5 d later but recovered faster within 10 d. The time course corresponded well with the slower establishment and quicker decay of long-lasting memory induced by massed training. The tight correlation observed between the structural modifications and the kinetics of long-lasting memory pinpoints the distinct temporal regulation of synaptic connections as a mechanism underlying the spacing effect.

Results

Memory Retention but Not Acquisition Is Dependent on the Length of Resting Intervals During HOKR Adaptation. A previous study has reported spacing effect on the retention but not on the acquisition of HOKR adaptation (12). Resting intervals of 60 min or longer resulted in a similar retention of HOKR gain after 24 h. Therefore, we tested resting intervals shorter or equal to 60 min within a constant total amount of training to study the effects of various temporal features of the stimulus on HOKR adaptation. Mice were trained to induce HOKR adaptation (Movie S1) for 1 h at 0.25 Hz with 17° oscillations of the screen (maximum screen velocity, 13.3°/s). Mice were either trained continuously using 900 cycles of massed training (M) or four sessions of 225 cycles each (15 min × 4) with varying intervals [spaced training (S)], 10 min (S_{10}, $n = 6$), 20 min (S_{20}), 40 min (S_{40}), or 60 min (S_{60}). The completion of each training required 1.5, 2, 3, and 4 h, respectively. The mice were kept in the dark in their home cages during the intervals and after training sessions to avoid additional visual input (Fig. 1*A*). The initial HOKR gain at the start of training was similar across all groups [Table S1; $P = 0.34$, $F(6, 44) = 1.030$, one-way ANOVA]. The HOKR gain increase was normalized to the initial gain. We explored the effects of M and S_{60} trainings on acquisition at the end of the HOKR training session and on retention on day 2 after the session. The increase in HOKR gain at the end of the 1-h training was significant [95–97%; $P < 0.001$, $F(2,19) = 8.83$, one-way ANOVA] and similar between the two groups, nearly reaching the saturated level of HOKR gain (Table S1 and Fig. 1 *B–D*). Obvious increments in HOKR gain were also observed during the intervals between the sessions of the spaced training (Fig. 1*C*). A further increase in gain was observed on day 2 after the S_{60} training, whereas massed training resulted in a significant decrease in HOKR gain (S_{60}, $P = 0.033$; M, $P = 0.021$, paired t test; Fig. 1 *B* and *D*). A similar acquisition and different retention of HOKR gain resulting from massed and spaced training were reproducible in a training condition in which the total training time was reduced to 0.5 h (Fig. S1 and Table S1), which confirmed that the increased retention afforded by S_{60} compared with M training was not due to a greater acquisition masked by the saturation of learning.

Next, we examined the influence of the duration of resting intervals on the acquisition and retention of the HOKR adaptation. The intervals tested (10, 20, 40, and 60 min) resulted in similar gain increases at the end of training and hence similar acquisition of short-term memory (Fig. 1*E* and S1*A*). However, the level of HOKR gain retention increased with wider intervals (Fig. 1*F*). S_{10} and S_{20} produced significant reductions in gain compared with that observed at the end of training on day 2, whereas that afforded by S_{40} remained unchanged, and that afforded by S_{60} significantly increased (S_{10}, $P = 0.005$; S_{20}, $P = 0.02$; S_{40}, $P = 0.1$; S_{60}, $P = 0.03$; paired t test; Table S1). Gain retention by S_{10} was notably similar to that of M training ($P > 0.1$, t test). These results indicate that the length of the resting interval between training sessions is critical for efficient memory retention and that a 1-h interval is sufficient to achieve the optimal long-term adaptation of HOKR.

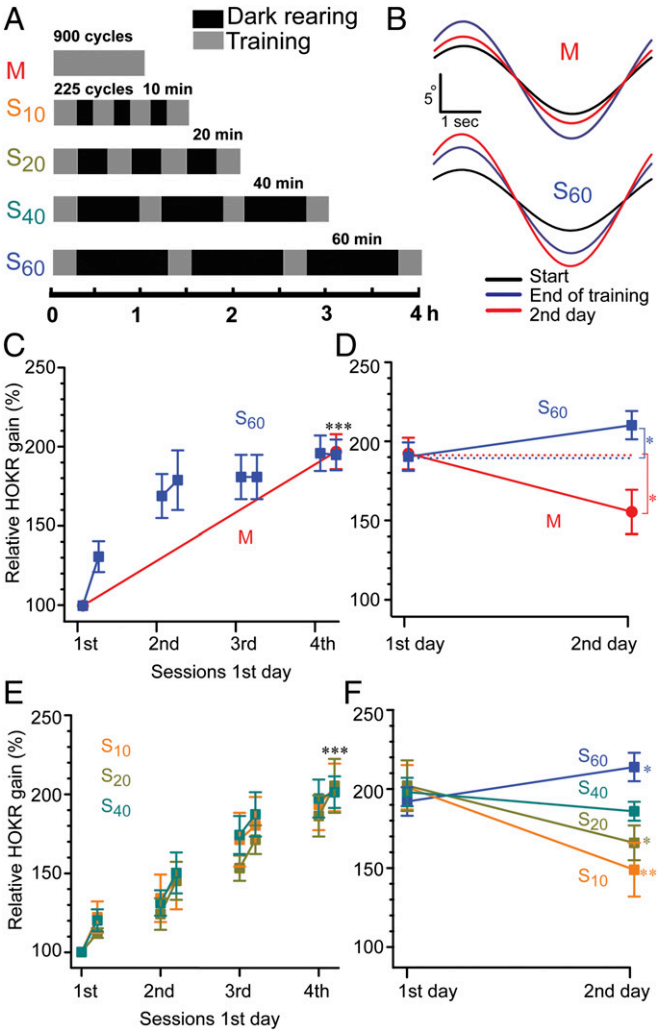

Fig. 1. Similar HOKR gain increase at the end of training but distinct retention on day 2 by massed or spaced training. (*A*) Protocols for HOKR training at 0.25 Hz, 17° screen oscillations. Mice received 900 cycles of 1 h massed (M; red) or 225 cycles × 4 of spaced (S) training with intervals of 10 min (S_{10}; orange), 20 min (S_{20}; dark yellow), 40 min (S_{40}; green), or 60 min (S_{60}; blue). Time taken to complete each protocol is shown in hours below. (*B*) Representative eye traces from individual animals at the start (black), at the end (blue), and on day 2 (red) after the 1-h training. (*C*) Similar HOKR gain increase (%) by M ($n = 10$) and S_{60} ($n = 9$). (*D*) Relative gain increases at the end of training (day 1) and on day 2 indicating retention of HOKR adaptation after 24 h. (*E* and *F*) Similar to *C* and *D* but for shorter resting intervals of S_{10}, S_{20}, and S_{40} ($n = 6–9$). ***$P < 0.001$ vs. initial gain, one-way ANOVA. (*D* and *F*) *$P < 0.05$, **$P < 0.01$ vs. end of training on day 1, paired t test.

Distinct Modification of PF–PC Synapses During Acquisition of Memory With or Without Intervals. Because the spaced training produced improved retention along with similar acquisition of HOKR gain compared with massed training, we examined whether any differences in the structural modifications at PF–PC synapses could be detected. We previously showed that HOKR adaptation at the end of 1 h of continuous (massed) training induced a reduction in the number of AMPA-type glutamate receptors (AMPARs) in the middle part of the Fl. However, there was no alteration in the size of postsynaptic densities (PSDs) or the number of PF–PC synapses (30). The reduction in the number of AMPARs recovered within 24 h and was followed by a reduction of PF–PC synapses. The reduction of synapses was specifically induced in the middle but not rostral or caudal Fl, which is consistent with a functional mapping study performed in the mouse that showed PCs located in zone 2 (middle Fl) but not zone 1 (caudal Fl) and zone 3 (rostral Fl) responding to the horizontal movement of visual stimuli in mouse (34).

Here, using the most efficient spaced training protocol (S_{60}), the density of AMPARs in individual PF–PC synapses and the sizes of PSD and spines were measured by electron microscopy (EM). We found a significant reduction in AMPAR-labeling density at the end of training (4 h, Fig. 2*B*) in the Fl compared with the adjacent paraflocculus (Pfl) (25% reduction on average; Fl, 150 ± 13.6/μm^2; Pfl, 198 ± 7.9/μm^2; $n = 5$ for each; $P = 0.009$, paired t test; Fig. 2 *A* and *B*), which was similar to the AMPAR density reduction produced by massed training (28%) (30). However, at 4 h after the spaced training (8 h), AMPAR density in the Fl was not different from that observed in the Pfl (Fig. 2*B*; Fl, 41.6 ± 3.9/μm^2; Pfl, 40.8 ± 3.8/μm^2; $n = 5$ for each; $P = 0.67$, paired t test). At all time points, the postsynaptic IMP cluster areas sampled in the Fl (0 h, 0.044 ± 0.0030/μm^2; 4 h, 0.045 ± 0.0034/μm^2; 8 h, 0.039 ± 0.0014/μm^2) and Pfl (0 h, 0.041 ± 0.0014/μm^2; 4 h, 0.041 ± 0.0024/μm^2; 8 h, 0.042 ± 0.0010/μm^2) were not different ($P > 0.23$, Student t test). Next, we examined the PSD lengths from single EM sections in S_{60} ($n = 3$ animals, $n = 300$ PSDs for all groups; Fig. 2 *C–F*). We found a significant decrease in the Fl at the end of training (4 h, 0.20 ± 0.004 μm; $P < 0.001$) and 1 h after training [5 h, 0.22 ± 0.004 μm; $P = 0.008$, Mann–Whitney U (MWU) test] compared with the untrained control Fl (0.24 ± 0.005 μm). No changes were detected in the Fl at 4 h after training (8 h) or on day 2 (24 h), or in the Pfl, at any of the examined time points. We further examined the PSD area and PC spine volume in serial sections from the Fl at the end of the S_{60}, a time at which the maximum decrease in PSD length was detected in the single-section analysis (Fig. 3). Cumulative curves of PSD area and spine volume (Fig. 3 *B* and *C*) showed significant leftward shifts compared with the Fl of the untrained control (PSD area: 4 h, 0.068 ± 0.003 μm^2; control, 0.089 ± 0.004 μm^2, $P = 0.024$, spine volume: 4 h, 0.080 ± 0.002 μm^3; control, 0.10 ± 0.004 μm^3, $P = 0.012$, K–S test, $n = 60$ for each group), indicating that the major population of synapses was reduced with regard to both PSD area (23%) and spine volume (20%). No naked spines (without PSDs) were observed in the trained sample ($n = 150$), suggesting a tight coupling between the shrinkage of PSDs and spines. We found a positive correlation between PSD area and spine volume in the trained group ($r = 0.66$, $P < 0.001$, Pearson correlation) that was similar to that of the control ($r = 0.55$, $P < 0.001$, Pearson correlation, Fig. 3*D*). These results indicate the shrinkage of the PF–PC synapses and spines during cerebellar motor learning. Despite the similar gain increases observed at the end of training, the synaptic modifications during the acquisition of memory were different between massed and spaced training.

Memory Retention Is Strongly Correlated with Reductions in PF–PC Synapses. We further explored the structural basis of differential memory retention with distinct intervals and examined the correlation between the number of PF–PC synapses and the retention

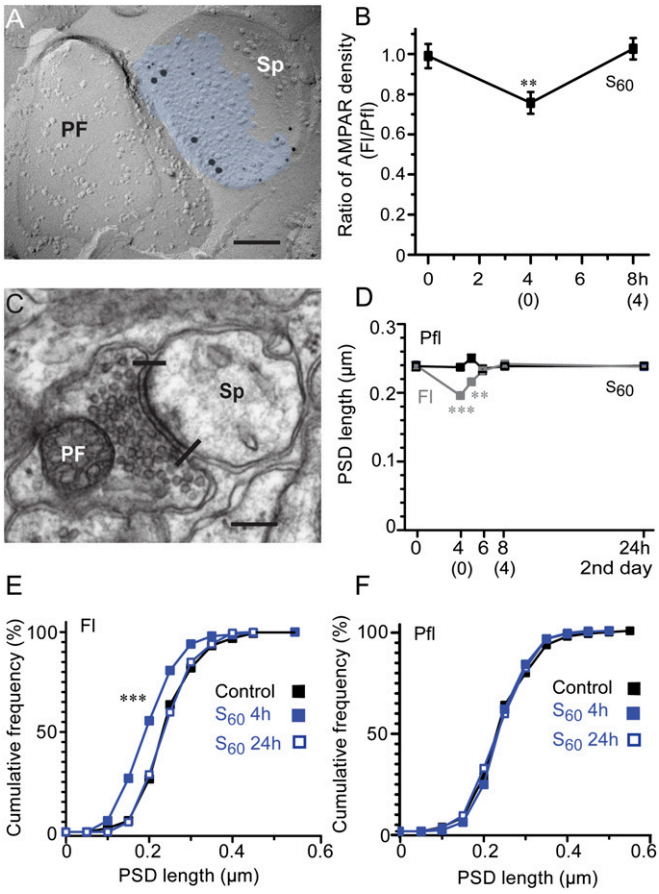

Fig. 2. Immediate reduction in AMPAR density at PF–PC synapses in Fl and their shrinkage during acquisition of HOKR adaptation by spaced training. (*A*) An EM image of replica immunolabeled for AMPARs (5-nm particles) in PF–PC spine synapse (Sp) identified by labeling for GluD2 (15-nm particles). The density of AMPAR labeling is calculated by dividing the number of immunogolds for AMPARs/synapse with area of intramembrane particle clusters (blue). (*B*) Pooled data showing significant reduction of AMPAR density after training (4 h) but not at 4 h after training (8 h) in S_{60} training. (0) and (4) on *x* axis represent time after training. Ratios of AMPAR density in Fl compared with those in Pfl are shown ($n = 5$ each, $^{**}P < 0.01$, paired t test). (*C*) PF–PC synapse showing PSD length in single ultrathin sections (edges indicated by lines). (*D*) Time course of changes in PSD length shows significant shrinkage at the end of training (4 h) and 1 h after S_{60} training with no change at 4 h after training (8 h) and on day 2 (24 h) in Fl (4 h, $^{***}P < 0.001$; 5 h, $^{**}P < 0.01$; $n = 300$ for all, MWU test). (*E*) Significant leftward shift of cumulative distributions of PSD length in Fl detected at S_{60} 4 h (blue filled square; $^{***}P < 0.001$, two-sample K–S test) but not at S_{60} 24 h (blue open square) compared with control (black filled square). (*F*) No change was detected at any time points in Pfl. (Scale bar, 0.2 μm in *A* and *C*.)

of HOKR gain on day 2. The density of these synapses in the superficial molecular layer of the middle part of the Fl and the adjacent Pfl was measured using the unbiased physical dissector method in M, S_{40}, and S_{60} mice (Fig. 4). We observed a significant reduction in PF–PC synapses after massed (0.73 ± 0.05 synapses/μm^2, –26%, $n = 5$) and spaced (S_{40}, 0.58 ± 0.02 synapses/μm^2, –41%, $n = 3$; S_{60}, 0.47 ± 0.005 synapses/μm^2, –53%, $n = 3$) trainings compared with the untrained control Fl [0.99 ± 0.005 synapses/μm^2, $n = 5$; $P < 0.001$ for all, $F(3,12) = 65.6$, one-way ANOVA, Tukey's post hoc test; Fig. 4*B*]. No differences were detected in the Pfl of any of the groups. Volumetric analysis of the molecular layer did not reveal any change in the volume of the Fl in the trained group (S_{60}, 0.26 ± 0.005 mm^3, $n = 5$) compared with the control (0.25 ± 0.006 mm^3, $n = 5$; Fig. S2). The mean of the

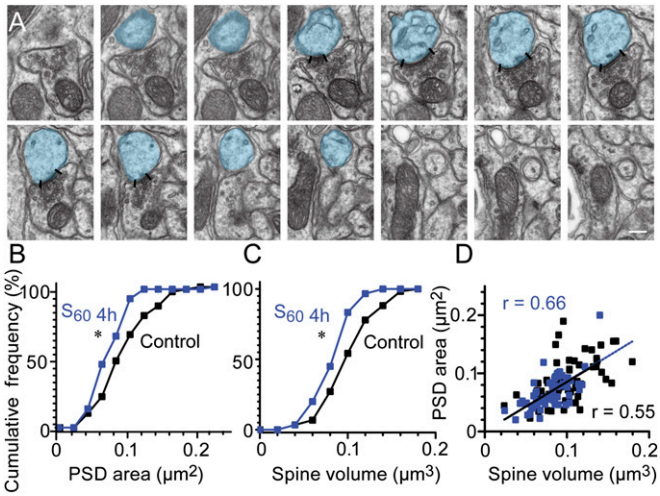

Fig. 3. Simultaneous shrinkage of synapse and PC spine at the end of spaced training. (*A*) Serial EM images of a PC spine used to measure PSD area (edges indicated by lines) and PC spine head (blue) volume. Last three serial sections represent the neck of spine and were not used for spine head volume estimation. (Scale bar, 0.2 μm.) (*B* and *C*) Cumulative frequency plots showing significantly smaller PSD (leftward shift) (*B*) and spine size (*C*) just after the completion of S_{60} training (S_{60} 4 h, $n = 60$; blue) compared with control (black; $n = 60$, $^{*}P < 0.05$, two-sample K–S test). (*D*) Scatter plot showing positive correlation of the spine head volume and PSD area in both control and S_{60} 4 h (control, $r = 0.55$, black line; S_{60} 4 h, $r = 0.66$, dashed blue line; $^{***}P < 0.001$ for both groups, Pearson correlation).

Fl/Pfl synapse density ratios in the M, S_{40}, and S_{60} groups exhibited a strong negative correlation with the mean of the HOKR retention ratios (gain increase on day 2/end of the training, $r = 0.97$, $P < 0.001$, Pearson correlation; Fig. 4*C*). The tight correlation observed between the reduction of the PF–PC synapses and the retention of HOKR gain suggests that synaptic structural plasticity in the cerebellar cortex is a physical substrate of long-lasting memory.

Differential Time Course of the Formation and Decay of Long-Lasting Memory Between Massed and Spaced Learning. To further substantiate this conclusion, we compared the massed and spaced training protocols with regard to the time course of the development and decay of memory after a single learning event (Fig. 5). Mice were subjected to a 1-h massed (M) or spaced (S_{60}) training. The HOKR gain increase retained on day 2 in the S_{60} group was significantly maintained for 27 d and gradually recovered by 7 wk. In contrast, the reduced gain observed in the M group on day 2 unexpectedly developed again and reached a level that was not significantly different from that of the S_{60} group on day 5. However, the increased gain of the M group on day 5 quickly decayed within 2 wk. This HOKR gain increase on day 5 in the M group was similar in the presence or absence of 1 min of recording on day 2 (Fig. S3). This indicated that the regain of memory was not due to the brief exposure to the stimulus but due to the slow development of memory induced by 1 h of massed training. These results demonstrated that massed training can induce long-lasting memory of similar strength but slower formation and quicker decay compared with that induced by spaced training. Thus, the temporal pattern of training is an essential determinant of the kinetics of long-lasting but not short-lasting memory.

Tight Correlation Between the Time Courses of Structural Plasticity and Long-Lasting Memory. Further, we examined the correlation between the time courses of the structural changes observed in PF–PC synapses and long-lasting memory after M and S_{60} training (Fig. 6). The S_{60} group exhibited a significant but small reduction in synaptic density at the end of training (4 h, 0.88 ± 0.01 synapses/μm^2, −11%, $n = 3$), which reached a peak at 4 h after the training (8 h, 0.43 ± 0.01 synapses/μm^2, −57%, $n = 3$) when reduction of AMPARs and shrinkage in PSD area recovered. This reduction was maintained until at least day 15 [0.54 ± 0.02 synapses/μm^2, −46%, $n = 3$, $P < 0.001$ for all, $F(4, 12) = 546$, one-way ANOVA, Tukey's post hoc test] and was tightly correlated with the gain increase. Thus, 4 h after spaced training, a time at which the reduction of AMPARs and shrinkage in PSD area recovered, 50% of PF–PC synapses had already been eliminated. The reduction of synapses observed in the M group also correlated well with the behavior, peaking on day 5 [0.491 ± 0.04 synapses/μm^2, −50%, $n = 3$, $P < 0.001$, $F(3,12) = 58.6$, one-way ANOVA, Tukey's post hoc test] and recovering on day 15 (1.09 ± 0.037 synapses/μm^2, $n = 3$, $P = 0.24$). Taken together, these results illustrate a tight correlation of structural changes of PF–PC synapses with the HOKR gain increase.

PC Spine Changes Concurrent with Synapse Reduction and Recovery. Because spaced training rapidly reduced PF–PC synapses within 4 h after training, we examined whether this acute change was accompanied by PC spine elimination by measuring the spine

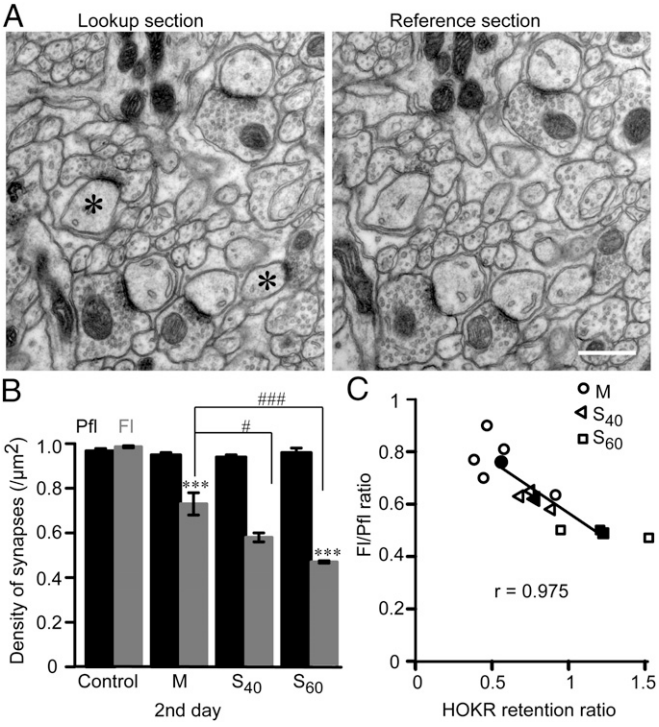

Fig. 4. Strong negative correlation between reduction of PF–PC synapses in Fl and retention of HOKR gain on the second day. (*A*) Consecutive EM sections (thickness of 70 nm) were used for measurement of PF–PC synapse density using physical dissector method. Synapses present in lookup section but not in the reference section were counted (*). (Scale bar, 0.5 μm.) (*B*) Significant reduction of PF–PC synapse density in Fl (gray) on day 2 but not in Pfl (black) following M ($n = 5$), S_{40} ($n = 3$), and S_{60} ($n = 3$) trainings ($^{***}P <$ 0.001 vs. control Fl, $n = 5$, one-way ANOVA). The reduction of synapse density by M is still significantly smaller than S_{40} ($^{\#}P < 0.05$) and S_{60} ($^{\#\#\#}P <$ 0.001, one-way ANOVA) showing interval-dependent synapse reduction. (*C*) Scatter plot showing a strong negative correlation between PF–PC synapse density (Fl/Pfl ratio) and HOKR retention ratio (ratio of HOKR gain increase on day 2 to that at the end of training, $r = 0.975$, $P < 0.001$, Pearson correlation). Data from individual animals (open) and the mean (filled) from M (circle), S_{40} (triangle), and S_{60} (square) were plotted. Regression line is obtained from means of three groups.

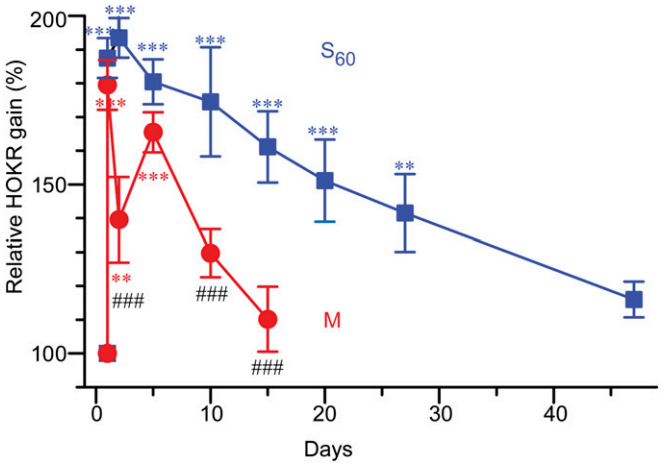

Fig. 5. Distinct kinetics of long-lasting memory in extended time course after massed or spaced training. HOKR gain increase observed on day 2 in S_{60} (dark blue; $n = 12$) was maintained over a month and reduced to a level not significantly different from the initial gain on day 47 (***$P < 0.001$, **$P < 0.01$, one-way ANOVA). On the other hand, the HOKR gain in M (red; $n = 15$) decreased on day 2 and increased again on day 5 (***$P < 0.001$, **$P < 0.01$, one-way ANOVA). The gain increase observed on day 5 in M was similar to that on day 2 in S_{60} ($P > 0.05$ vs. day 2 in S_{60}), thus showing delayed formation of long-lasting memory by M. Gains on days 2, 10, and 15 in M showed significant difference from that on day 2 in S_{60} ($^{###}P < 0.001$, one-way ANOVA).

density along PC dendrites using high-voltage EM (Fig. 7). We observed a dramatic loss of PC spines in the Fl, 4 h after the training and at 24 h [8 h, 3.7 ± 0.3 spines/μm, −35%; 24 h, 3.1 ± 0.2 spines/μm, −45%, $P < 0.001$ for all, $F(5,155) = 67.8$, one-way ANOVA, Tukey's post hoc test] compared with the dense spines observed in the untrained control Fl (5.7 ± 0.2 spines/μm). Pfl remained unchanged at all time points (control, 6.0 ± 0.1, 4 h; 6.1 ± 0.3, 8 h; 6.4 ± 0.3 spines/μm, $P > 0.85$). Similarly, the M group exhibited significant reduction in spine density in the Fl on day 5 [3.9 ± 0.03 spines/μm, −33%, $P < 0.001$, $F(2,172) = 76.8$, one-way ANOVA, Tukey's post hoc test]. On day 15, when the basal HOKR gain and synapses recovered in the M group, the spine density also recovered to a level that was comparable to that of the control (5.8 ± 0.03 spines/μm, +0.2%). A three-dimensional reconstruction of serial EM images also confirmed a similar recovery of spine density (control, 6.0 ± 0.39 spines/μm, $n = 12$; day 15, 5.9 ± 0.27 spines/μm, $n = 14$, $P > 0.33$, Student t test). Taken together, our results demonstrated that the synaptic modifications in the cerebellar cortex during motor memory formation emerge first as a reduction in AMPARs, followed by the shrinkage and the elimination of the PF–PC synapses and spines (Fig. 8).

Discussion

Our results demonstrated a strong correlation between the distinct temporal regulation of motor memory and alterations in PF–PC synapses and PC spines after massed and spaced training. The detailed study of the time course indicates that the structural modifications established within hours after the HOKR training are the synaptic mechanisms underlying the spacing effect. Rapid structural modifications of synaptic connections may be a common mechanism underlying a remarkably ubiquitous spacing effect. Moreover, we found that massed training can also induce a similar gain increase in long-term adaptation with slow formation and rapid decay kinetics. These findings suggest that the kinetics but not the amount of long-term memory is modulated by the spacing.

Memory induced by repeated training spaced over time is superior to an equal amount of training without spacing (9, 13). Ebbinghaus discovered the spacing effect in 1885, and since then, numerous models have been proposed to explain it. The benefits of this effect have been attributed to efficient acquisition of memory (35) and superior retention (36). Studies using an appetitive conditioning task and taste aversion learning in rats demonstrated that longer trial spacing facilitated the acquisition of memory (37, 38). In contrast, an odor avoidance task performed in *Drosophila*, sensitization of the gill withdrawal reflex in *Aplysia*, and place navigation task performed in rats have shown facilitation of memory retention by spacing (10, 16, 18). We also observed a selective influence of the spacing on retention but not acquisition of memory in HOKR adaptation (Fig. 1), which is consistent with the results of a previous study that was performed using a similar model (12). Thus, the spacing effect appears to occur selectively on acquisition or retention of memory depending on learning paradigms. Facilitation of the memory retention observed in our spaced HOKR training was interval-dependent in the range of 10–60 min intervals (Fig. 1*F*). A previous study using HOKR showed no significant difference in retention between 1-h and 24-h intervals (12). These results indicate that 1-h interval is critical and sufficient for maximal facilitation of memory retention in HOKR adaptation.

We extensively monitored changes in the HOKR gain for a few weeks after identical amounts of stimulus presentation for massed and spaced training. Massed training exhibited two peaks of HOKR gain increase: the first peak was observed at the end of training on day 1, followed by the second peak on day 5, which had a similar gain that decayed within a week. These two peaks were well correlated with AMPAR (30) and synapse reduction (Fig. 5), respectively. In a previous study, we repeated 1-h massed training for several days and observed a mixture of short-

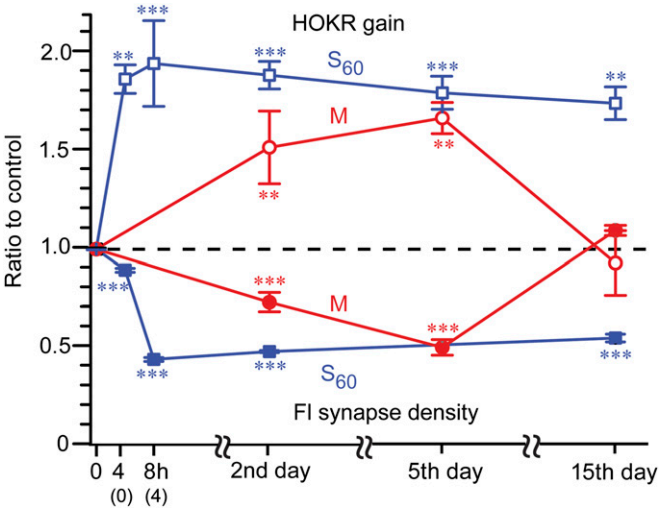

Fig. 6. Tightly correlated reduction of PF–PC synapses to the long-lasting memory by massed or spaced training. Time course of Fl synapse density in M (red; filled circles) and S_{60} (dark blue; filled squares) showed a mirror image of that of HOKR gain (open circles and squares, respectively) expressed as ratios to control. A slight but significant reduction in synapse density was already observed at the end of S_{60} training (4 h, $n = 3$), which completely developed within 4 h after S_{60} (8 h, $n = 3$) and was maintained at least until day 15 ($n = 3$, ***$P < 0.001$ vs. control Fl, one-way ANOVA). Mice trained by M training gradually developed a reduction in synapse density ($n = 3$, ***$P < 0.001$ vs. control Fl, one-way ANOVA) reaching a similar level on day 5 to that of 4 h after S_{60} and recovered to control level on day 15 ($n = 3$, $P > 0.05$). **$P < 0.01$, ***$P < 0.001$ vs. initial gain in control, one-way ANOVA. (0) and (4) on x axis represent time after training.

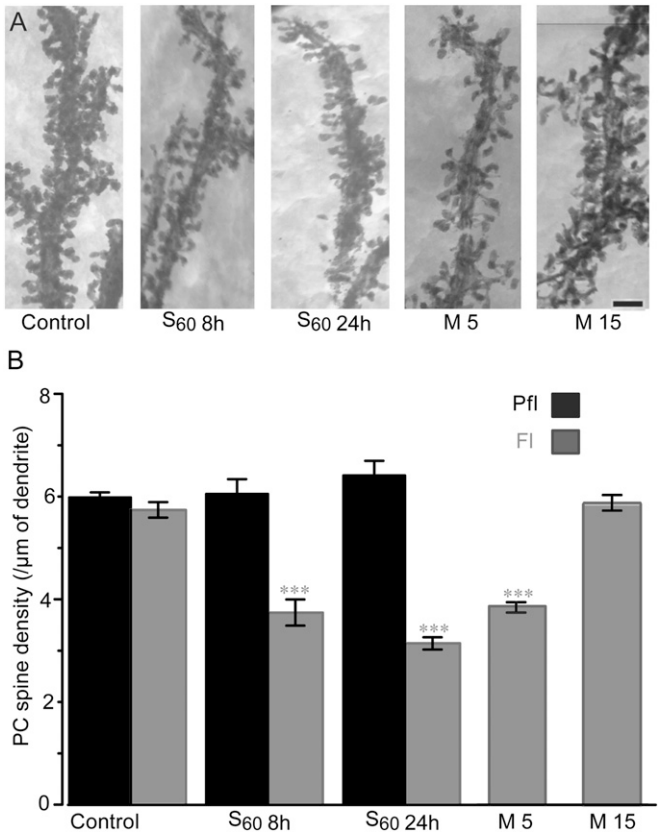

Fig. 7. Elimination and recovery of PC spines. (*A*) High-voltage EM images of PC dendrites in Fl in control, 4 h after S_{60} (8 h), on day 2 after S60 (24 h), on day 5 (M5), and on day 15 after M (M15). (Scale bar, 2 μm.) (*B*) Spine densities along PC dendrites showed robust PC spine elimination selectively in Fl (gray) but not in Pfl (black) at 4 h (S_{60} 8 h, $n = 5$) and 24 h (S_{60} 24 h, $n = 5$) after S_{60} training. After M training, a similar spine elimination was observed on day 5 (M5, $n = 3$) compared with control Fl ($n = 5$, $^{***}P < 0.001$ vs. control Fl), but it recovered on day 15 (M15, $n = 3$, $P = 0.99$ vs. control Fl).

term and long-term adaptations (30). In the present study, we clearly separated long-term adaptation and revealed its unforeseen slow development by single massed training. Thus, the reduction in HOKR gain after massed training on day 2 most likely reflects the rapid decay of the short-term memory and slow development of the long-term memory. Spaced training exhibited a single peak that was sustained for more than 4 wk. At the end of spaced training, we detected a transient reduction in AMPARs and shrinkage of synapses and spines, followed by persistent synapse elimination within 4 h. The rapid acquisition of short-term memory may be supported by AMPAR reduction in both massed and spaced trainings. However, it is conceivable that the apparent short-term adaptation at the end of spaced training already contains a component of long-term adaptation that rapidly develops with synapse elimination. Net AMPAR reduction in PF–PC synapses was maintained constant throughout the development of long-lasting memory; it is calculated to be 50% just after spaced training (75% AMPAR density × 77% synapse size × 88% synapse number) and also at 4 h after the training (50% synapse number with no change in AMPAR density and synapse size). The tight correlation between the decay of long-term adaptation and recovery from synapse reduction in both massed and spaced trainings also strengthens our notion that long-term memory is supported by synapse elimination (30). The reduction of PF–PC synapses may serve as a permissive mechanism for the memory transfer from the cerebellar cortex to vestibular nuclei (39).

What proportion of the population of PF–PC synapses in the middle part of the Fl is involved in HOKR learning? There are two possibilities: (*i*) 50% of the PF–PC synapses in the total population are involved and the remaining 50% are unchanged or (*ii*) the entire population of synapses undergoes changes followed by a recovery of 50%. The latter is more likely, considering the parallel shifts in the distributions of AMPAR numbers (30), PSD, and spine sizes (Figs. 2 and 3).

The spacing effect requires new protein synthesis (14, 40). In addition, a recent study has shown that the blockade of protein synthesis in the Fl with anisomycin abolished HOKR adaptation during spaced but not massed training (12). This is consistent with our study that showed rapid structural modifications in the Fl after spaced training, considering that new protein synthesis is necessary for the restructuring of synapses (2). In contrast, at the end of massed training, we observed only a reduction in AMPAR (30), which does not depend on new protein synthesis (41). HOKR adaptation on day 2 was not affected by anisomycin in either massed or spaced training (12). This is also consistent with our discovery of long-lasting structural changes, which could resume after the washout of anisomycin.

What is the mechanistic basis of the slow and rapid development of long-lasting memory in massed and spaced training? A *Drosophila* study showed that repetitive peaks of MAP kinase activity occur only during resting intervals and that continuous training induced only one peak in MAP kinase activity 20 min after the end of training (21). Repetitive peaks in MAP kinase activation may lead to rapid structural modifications and the development of long-lasting memory observed after spaced training, whereas gradual increases over long periods after massed training may induce the slow formation of long-lasting

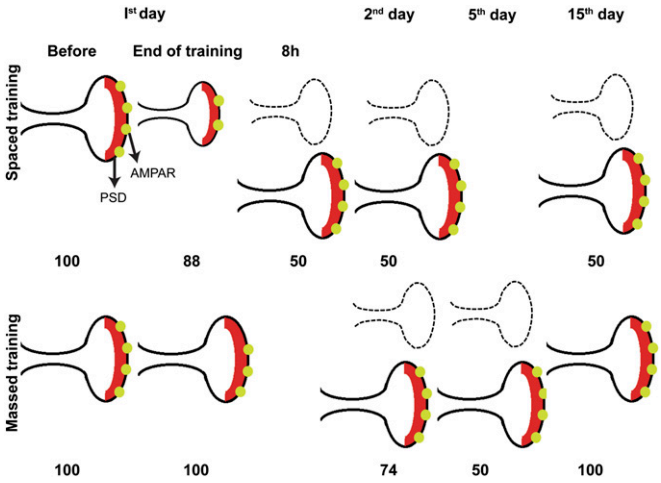

Fig. 8. Schematic diagram of the time courses and sequential steps of synaptic plasticity at PF–PC synapses after spaced and massed trainings. Numbers represent the percentages of PF–PC synapses relative to the untrained control. The spines indicated by dotted lines disappeared at the observed time points. Immediate HOKR adaptation after massed training resulted in a reduction in AMPARs (28%) but no structural changes, whereas spaced training produced shrinkage in PSDs (23%) and spine size (20%) with a reduction in AMPAR density (25%) by the end of training. The rapid structural changes observed in spaced training were fully established as a 50% reduction in PC synapses and spines within 4 h after training and were maintained at least for 2 wk. By contrast, massed training slowly produced a 50% synapse reduction by the fifth day that recovered rapidly within 2 wk. Our results strongly suggest distinct structural plasticity in synapses as a subcellular correlate for differential kinetics of memory in massed and spaced learning.

memory. Surprisingly, even after the acquisition of similar levels of behavioral gain and synaptic elimination, the long-lasting memory decayed much quicker in massed than in spaced training. It is believed that memory is supported by the balance between the formation and recovery processes (42). Previous studies have shown that kinases (43, 44) and phosphatases (33) act as switches of synaptic plasticity, thus regulating memory formation and reversal processes (45, 46). Thus, the slow formation of memory by massed training may allow strong reversal processes and induce the rapid decay of long-lasting memory, whereas the rapid formation of memory observed in spaced training may strongly suppress reversal processes.

Memory incubation, which is the enhancement of memory over time in the absence of additional training, is observed across several behavioral paradigms (47, 48). We also observed an increment in HOKR gain during the resting intervals in all spaced training protocols and across several hours or days after completion of spaced or massed training, respectively. However, little is known about the mechanisms underlying memory incubation. One possibility is that posttraining reactivation of activity patterns contributes to the incubation by promoting the efficient restructuring of synapses and the remodeling of neuronal circuits (49). Thus, such "activity replay" may occur over several hours or days after spaced or massed training, through distinct kinetics of synaptic remodeling. Repetitive training including 1-h intervals may result in cumulative memory incubation and rapid structural modifications in spaced training.

Further investigations are needed to elucidate the precise molecular mechanisms that regulate the temporal features of long-lasting memory, and the structural modification of synapses provides an indispensable readout for such studies.

Materials and Methods

HOKR Setup and Eye Movement Recordings. C57BL/6NJcl male mice (13–16 wk old) were used in this study. All of the animal experiments were approved by the Animal Care and Use Committee of National Institute for Physiological Sciences. Efforts were made to minimize the animal suffering and number of animals. Mice were housed individually for more than 7 d under standard laboratory conditions with food and water ad libitum. Under pentobarbital anesthesia (50 mg/kg, i.p.) and aseptic conditions, a screw (6 mm head diameter and 10 mm length) was attached to the cranial bone of mice between lambda and bregma using synthetic resin (Super bond C&B; Sun Medical). The animals were allowed to recover for at least 42 h after the operation. Parameters of the HOKR setup have been modified from previous studies (50) to maximize the gain increase (from 30% to 40% in ref. 30 to 100% in the present study) as follows. Each mouse was mounted on a stage with head fixed and its body loosely restrained in an upward sloping plastic cylinder so that the head was positioned for maximum visual input. The stage was surrounded by checked-pattern (check size, 3.2°) cylindrical screen 64 cm in diameter (50). The illumination on the screen was adjusted to 80–100 lx for better visualization and adequate size of the pupil for better image processing and detection of the eye movement (Movie S1). Mice were kept alert and awake through exposure to white noise sounds during training sessions. These conditions increased the visual inputs and hence retinal slip sensitivity and alertness of animals, thus facilitating learning of HOKR in the mice. The change of C57BL/6 substrain (from j to Njcl) also contributed to less variability among animals compared with our previous study (30). Movements of the right eye were monitored with high-speed analog CCD camera (CS3720; Toshiba TELI) placed at an angle of 60° laterally from the midline and 30° down from the horizontal plane (51). Infrared light-emitting diodes (HSDL4230; Agilent Technologies) attached to the camera illuminated the eye with wavelength of 880 nm, which was displayed on the monitor. The real-time position of the eye was measured by image processing software written in LabVIEW using IMAQ Vision (National Instruments) (51). The HOKR was induced by sinusoidal oscillations of the screen by 17° (peak-to-peak) at 0.25 Hz (maximum screen velocity 13.3°/s). Over 10 cycles of evoked smooth pursuit eye movements free from saccades and blinks were selected and averaged to calculate the mean amplitude. HOKR gain was defined as a ratio of the amplitude of the eye movement to that of screen oscillation (peak-to-peak).

HOKR Training Schedules. HOKR adaptation was examined by massed and spaced training paradigms. Total duration of the HOKR training was kept either 1 h or 0.5 h with constant screen oscillations by 17° at 0.25 Hz. Mice were randomly assigned to one of the two training paradigms. For the M training paradigm, mice received either 900 cycles or 450 cycles of continuous training without any resting interval. For the S training paradigm, for 1-h training, mice received four training sessions of 225 cycles (15 min) with increasing intervals of 10 min (S_{10}), 20 min (S_{20}), 40 min (S_{40}), and 60 min (S_{60}), taking 1.5, 2, 3, and 4 h, respectively, to complete the training. For 0.5-h training, mice received four sessions of 112.5 cycles (7.5 min) with intervals of 60 min ($S_{60}0.5$). It took 3.5 h to complete the training. HOKR gain was measured by initial and last 75 cycles (5 min) of eye movements for each training session. On subsequent days after the training, 20 cycles of eye movement were recorded to measure the HOKR gain. Mice were kept in home cages in the dark during resting periods in spaced training.

Volume Measurement of Floccular Molecular Layer. To measure the volume of molecular layer in untrained control and trained animals, 60-μm serial sections containing the whole Fl were mounted on the glass slides and processed for Nissl staining with cresyl violet (30). Sections were photographed using a DP70 digital camera affixed to a BX50 light microscope (Olympus).

Measurement of AMPA Receptor Density in PF–PC Synapses. SDS-digested freeze-fracture replica labeling was used to estimate the density of AMPARs as described in our previous study (52). Briefly, under sodium pentobarbital (50 mg/kg, i.p.) anesthesia, mice were perfused. Cerebella (including Fl and Pfl) were cut into 120-μm-thick slices with a microslicer (DTK-1000; Dosaka) and cryoprotected with 30% (wt/vol) glycerol in PBS for 12–16 h. The slices through Fl and Pfl at the middle of rostro–caudal axis were trimmed out, frozen with a high-pressure freezing machine (HPM010; BAL-TEC), and fractured in a freeze-fracture machine (BAF 060; BAL-TEC). The exposed membrane faces were replicated by carbon (5 nm) and platinum/carbon (2 nm) followed by carbon (15 nm). The replicas were transferred to 2.5% (wt/vol) SDS containing 0.0625 M Tris·HCl and 10% (wt/vol) glycerol, pH 6.8, and incubated for 18 h at 80 °C. After the treatment with SDS, replicas were washed and blocked for 1 h with 5% (wt/vol) BSA in Tris-buffered saline (TBS). The replicas were then reacted with rabbit polyclonal antibody for pan-AMPA (6.7 μg/mL) (53) and guinea pig polyclonal antibody for GluD2 (0.55 μg/mL) (53), which was used to mark PF–PC synapses, at 15 °C for 48 h. The replicas were then washed three times with 0.05% BSA in TBS, blocked with 5% BSA in TBS for 30 min, and incubated for 1 h at room temperature, followed by 24 h at 15 °C with the secondary antibodies in 5% BSA/TBS (1:20 dilution), goat anti-rabbit IgG coupled to 5-nm gold particles (British Biocell International) for AMPARs and goat anti-guinea pig IgG coupled to 15-nm gold particles (GE Healthcare) for GluD2 receptors. Replicas were first reacted with pan-AMPA antibody and its secondary antibody followed by incubation in the GluD2 receptor antibody and its secondary antibody. After immunogold labeling, the replicas were picked up onto grids coated with pioloform (Agar Scientific). Replicas were observed under a Tecnai 10 electron microscope (FEI Company) and photographed at 96,000× magnification. Immunogold particles within 30 nm from the edge of synaptic sites were included in the analysis because they can be distant from the epitope. The outline of synaptic sites was demarcated freehand, and their areas were measured by iTEM software (Olympus Soft Imaging Solutions). The density of receptors was then estimated by dividing the number of gold particles by the size of the postsynaptic area.

Measurements of PSD Size and Spine Head Volume. PSD length was measured on single EM sections. PSD area and spine head volume were traced from 15 to 20 serial ultrathin sections photographed at 12,500× magnification. The profile was defined as neck if minimum diameter was <200 nm and it remained unchanged in consecutive sections and was not included in spine head measurement (54). PSD area and spine head volume were calculated by summing the lengths of the PSD and spine head areas and multiplying by section thickness (70 nm), respectively.

Measurement of Density of PF–PC Synapses. Mice were intracardially perfused with PBS followed by fixative (0.8% paraformaldehyde, 1.5% glutaraldehyde in 0.1 M PB, pH 7.4). Brains were cut into 60-μm-thick coronal sections on a microslicer (VT 1000S; Leica). Sections were treated with 1% OsO_4, dehydrated and flat-embedded in durcupan resin (Fluka; Sigma-Aldrich), and polymerized at 60 °C. Serial ultrathin sections containing Fl at the middle of rostro–caudal axis were used for analysis. Adjacent Pfl was taken as an internal control because of no change in synapse number after HOKR training was observed (30). Sections were cut with an ultramicrotome (Reichert

Ultracut UCT; Leica) at the thickness of 70 nm and were collected on piolofrom-coated single-slot grids and contrasted by uranyl acetate and lead citrate. Pairs of micrograph from two consecutive sections were taken at 9,800× using a Tecnai 10 electron microscope. PF–PC synapses were identified by the presence of thick and prominent PSD in spines with small, rounded, axonal profiles containing loosely packed vesicles (55) in the superficial one third of the molecular layer. Synapse density was counted in a volume of 120 ± 15 μm^3 for each animal. The physical dissector was used for estimation of synapse density (56). The mathematical formula for calculation of the numerical density is as follows: density of synapse = Nsyn/tA, where Nsyn is the total number of synapses found only in the lookup sections, t is the section thickness (distance between the two sections), and A is the area of the counting frame.

Measurement of PC Spine Density. For the quantitative analyses of PC spine density, a rapid Golgi impregnation method was adopted as described previously (57). Briefly, after perfusion, the cerebella were dissected, and coronal 2–3 mm slabs were stored in the same fixative overnight at 4 °C. After washing with 0.1 M cacodylate buffer, the slabs were immersed in a mixture of 2.25% potassium dichromate and 0.4% osmium tetroxide for 4 d at 20 °C in darkness and stored in 0.75% silver nitrate solution for 3 d at 20 °C in dark. After gradual dehydration in alcohol, the tissues were transferred into propylene oxide, and embedded in an Epon mixture. Coronal 100-μm sections were made with a microtome and then reembedded on glass slides. Five-μm sections were made with an ultramicrotome mounted on 75 mesh double copper grids and observed under the Hitachi H-1250M high-voltage electron microscope (Hitachi). Distal dendrites of Purkinje cells were randomly photographed at a magnification of 3,000× and at the angles of 0° and ±8°-tilted for stereoscopical viewing. Spine density was calculated by dividing the number of spines by the length of the dendritic segment analyzed. In addition to the stereo images of Golgi-stained PCs, three-dimensional reconstruction of serial EM images (50 nm) was also used to count the number of spines along dendritic segments.

Quantitative and Statistical Analysis. iTEM software (Olympus-SIS) calibrated with a calibration grid (Ted Pella) was used for analysis of all images. Statistical analysis was performed using SPSS software (SPSS Inc.). Shapiro–Wilk's W test was applied for checking the normality of the datasets. The statistical significance was analyzed by paired *t* test within a group and by two-tailed unpaired Student *t* test and Mann–Whitney *u* test for comparison between two groups for parametric and nonparametric analyses, respectively. One-way ANOVA was used for statistical comparison among multiple groups. Tukey's post hoc test was further applied to allow the comparison of the mean of each group with the mean of the control group. For the comparison of cumulative frequency distributions, Kolmogorov–Smirnov test was used. Correlation analysis was performed using Pearson correlation test. Statistical significance was defined as $P < 0.05$. All of the data are expressed as mean ± SEM. "*n*" indicates number of animals.

ACKNOWLEDGMENTS. We thank Elek Molar for pan AMPAR antibody. We are grateful to Tomoya Sakatani for his help in setting up HOKR recording system and Etsuko Tarusawa and Naomi Kamasawa for their help in electron microscopy. We also thank Ko Matsui and Soichi Nagao for helpful discussion, Tatsuo Arii and Kazuyoshi Murata for the use of high-voltage electron microscope, and Sachiko Yamada and Ming-Zhu Zhai for the technical assistance. W.A. received scholarships for doctoral studies from Ministry of Education, Culture, Sports Science and Technology, Japan, and College Women Association of Japan. This work was supported by Solution Oriented Research for Science and Technology (R.S.), Core Research for Evolutional Science and Technology, Japan Science and Technology Agency (Y.F.), and Grants-in-Aid for Scientific Research on Priority Areas-Molecular Brain Sciences 16300114 (to R.S.) and 18022043 (to Y.F.).

1. McGaugh JL (2000) Memory—A century of consolidation. *Science* 287(5451):248–251.
2. Kandel ER (2001) The molecular biology of memory storage: A dialogue between genes and synapses. *Science* 294(5544):1030–1038.
3. Moga DE, Shapiro ML, Morrison JH (2006) Bidirectional redistribution of AMPA but not NMDA receptors after perforant path simulation in the adult rat hippocampus in vivo. *Hippocampus* 16(11):990–1003.
4. Lee S-JR, Escobedo-Lozoya Y, Szatmari EM, Yasuda R (2009) Activation of CaMKII in single dendritic spines during long-term potentiation. *Nature* 458(7236):299–304.
5. Lee HK, Kirkwood A (2011) AMPA receptor regulation during synaptic plasticity in hippocampus and neocortex. *Semin Cell Dev Biol* 22(5):514–520.
6. Bailey CH, Kandel ER (1993) Structural changes accompanying memory storage. *Annu Rev Physiol* 55(1):397–426.
7. Geinisman Y (2000) Structural synaptic modifications associated with hippocampal LTP and behavioral learning. *Cereb Cortex* 10(10):952–962.
8. Gómez-Palacio-Schjetnan A, Escobar ML (2008) In vivo BDNF modulation of adult functional and morphological synaptic plasticity at hippocampal mossy fibers. *Neurosci Lett* 445(1):62–67.
9. Ebbinghaus H (1885) *A Contribution to Experimental Psychology* (Teachers College, Columbia University Press, New York).
10. Spreng M, Rossier J, Schenk F (2002) Spaced training facilitates long-term retention of place navigation in adult but not in adolescent rats. *Behav Brain Res* 128(1):103–108.
11. Commins S, Cunningham L, Harvey D, Walsh D (2003) Massed but not spaced training impairs spatial memory. *Behav Brain Res* 139(1–2):215–223.
12. Okamoto T, Endo S, Shirao T, Nagao S (2011) Role of cerebellar cortical protein synthesis in transfer of memory trace of cerebellum-dependent motor learning. *J Neurosci* 31(24):8958–8966.
13. Carew TJ, Pinsker HM, Kandel ER (1972) Long-term habituation of a defensive withdrawal reflex in aplysia. *Science* 175(4020):451–454.
14. Naqib F, Sossin WS, Farah CA (2012) Molecular determinants of the spacing effect. *Neural Plast* 2012:581291.
15. Philips GT, Ye X, Kopec AM (2013) MAPK establishes a molecular context that defines effective training patterns for long-term memory formation. *J Neurosci* 33(17):7565–7573.
16. Tully T, Preat T, Boynton SC, Del Vecchio M (1994) Genetic dissection of consolidated memory in Drosophila. *Cell* 79(1):35–47.
17. Yin JCP, Del Vecchio M, Zhou H, Tully T (1995) CREB as a memory modulator: induced expression of a dCREB2 activator isoform enhances long-term memory in Drosophila. *Cell* 81(1):107–115.
18. Sutton MA, Ide J, Masters SE, Carew TJ (2002) Interaction between amount and pattern of training in the induction of intermediate- and long-term memory for sensitization in aplysia. *Learn Mem* 9(1):29–40.
19. Josselyn SA, et al. (2001) Long-term memory is facilitated by cAMP response element-binding protein overexpression in the amygdala. *J Neurosci* 21(7):2404–2412.
20. Wu G-Y, Deisseroth K, Tsien RW (2001) Spaced stimuli stabilize MAPK pathway activation and its effects on dendritic morphology. *Nat Neurosci* 4(2):151–158.
21. Pagani MR, Oishi K, Gelb BD, Zhong Y (2009) The phosphatase SHP2 regulates the spacing effect for long-term memory induction. *Cell* 139(1):186–198.
22. Hawkins RD, Kandel ER, Bailey CH (2006) Molecular mechanisms of memory storage in Aplysia. *Biol Bull* 210(3):174–191.
23. Woo NH, Duffy SN, Abel T, Nguyen PV (2003) Temporal spacing of synaptic stimulation critically modulates the dependence of LTP on cyclic AMP-dependent protein kinase. *Hippocampus* 13(2):293–300.
24. Kramár EA, et al. (2012) Synaptic evidence for the efficacy of spaced learning. *Proc Natl Acad Sci USA* 109(13):5121–5126.
25. Nagao S (1988) Behavior of floccular Purkinje cells correlated with adaptation of horizontal optokinetic eye movement response in pigmented rabbits. *Exp Brain Res* 73(3):489–497.
26. Raymond JL (1998) Learning in the oculomotor system: From molecules to behavior. *Curr Opin Neurobiol* 8(6):770–776.
27. van Alphen AM, Stahl JS, De Zeeuw CI (2001) The dynamic characteristics of the mouse horizontal vestibulo-ocular and optokinetic response. *Brain Res* 890(2):296–305.
28. Katoh A, Kitazawa H, Itohara S, Nagao S (1998) Dynamic characteristics and adaptability of mouse vestibulo-ocular and optokinetic response eye movements and the role of the flocculo-olivary system revealed by chemical lesions. *Proc Natl Acad Sci USA* 95(13):7705–7710.
29. Shutoh F, et al. (2003) Role of protein kinase C family in the cerebellum-dependent adaptive learning of horizontal optokinetic response eye movements in mice. *Eur J Neurosci* 18(1):134–142.
30. Wang, et al. (2013) Distinct cerebellar engrams in short-term and long-term motor learning. *Proc Natl Acad USA* 110:E188–E193.
31. Schonewille M, et al. (2011) Reevaluating the role of LTD in cerebellar motor learning. *Neuron* 70(1):43–50.
32. Gao Z, van Beugen BJ, De Zeeuw CI (2012) Distributed synergistic plasticity and cerebellar learning. *Nat Rev Neurosci* 13(9):619–635.
33. Schonewille M, et al. (2010) Purkinje cell-specific knockout of the protein phosphatase PP2B impairs potentiation and cerebellar motor learning. *Neuron* 67(4):618–628.
34. Schonewille M, et al. (2006) Zonal organization of the mouse flocculus: Physiology, input, and output. *J Comp Neurol* 497(4):670–682.
35. Hintzman DL (1974) *Theoretical Implications of the Spacing Effect* (Lawrence Erlbaum Associates, Potomac, MD), pp 77–97.
36. Fishman EJK, Keller L, Atkinson RC (1968) Massed versus distributed practice in computerized spelling drills. *J Educ Psychol* 59(4):290–296.
37. Domjan M (1980) Effects of the intertrial interval on taste-aversion learning in rats. *Physiol Behav* 25(1):117–125.
38. Sunsay C, Bouton ME (2008) Analysis of a trial-spacing effect with relatively long intertrial intervals. *Learn Behav* 36(2):104–115.
39. Shutoh F, Ohki M, Kitazawa H, Itohara S, Nagao S (2006) Memory trace of motor learning shifts transsynaptically from cerebellar cortex to nuclei for consolidation. *Neuroscience* 139(2):767–777.
40. Scharf MT, et al. (2002) Protein synthesis is required for the enhancement of long-term potentiation and long-term memory by spaced training. *J Neurophysiol* 87(6):2770–2777.
41. Houpt TA, Berlin R (1999) Rapid, labile, and protein synthesis-independent short-term memory in conditioned taste aversion. *Learn Mem* 6(1):37–46.
42. Colbran RJ (2004) Protein phosphatases and calcium/calmodulin-dependent protein kinase II-dependent synaptic plasticity. *J Neurosci* 24(39):8404–8409.

43. De Zeeuw CI, et al. (1998) Expression of a protein kinase C inhibitor in Purkinje cells blocks cerebellar LTD and adaptation of the vestibulo-ocular reflex. *Neuron* 20(3): 495–508.
44. Feil R, et al. (2003) Impairment of LTD and cerebellar learning by Purkinje cell-specific ablation of cGMP-dependent protein kinase I. *J Cell Biol* 163(2):295–302.
45. van Woerden GM, et al. (2009) betaCaMKII controls the direction of plasticity at parallel fiber-Purkinje cell synapses. *Nat Neurosci* 12(7):823–825.
46. Jörntell H, Hansel C (2006) Synaptic memories upside down: Bidirectional plasticity at cerebellar parallel fiber-Purkinje cell synapses. *Neuron* 52(2):227–238.
47. Frankland PW, et al. (2004) Consolidation of CS and US representations in associative fear conditioning. *Hippocampus* 14(5):557–569.
48. Pickens CL, Golden SA, Adams-Deutsch T, Nair SG, Shaham Y (2009) Long-lasting incubation of conditioned fear in rats. *Biol Psychiatry* 65(10):881–886.
49. Cole CJ, et al. (2012) MEF2 negatively regulates learning-induced structural plasticity and memory formation. *Nat Neurosci* 15(9):1255–1264.
50. Nagao S (1983) Effects of vestibulocerebellar lesions upon dynamic characteristics and adaptation of vestibulo-ocular and optokinetic responses in pigmented rabbits. *Exp Brain Res* 53(1):36–46.
51. Sakatani T, Isa T (2004) PC-based high-speed video-oculography for measuring rapid eye movements in mice. *Neurosci Res* 49(1):123–131.
52. Tarusawa E, et al. (2009) Input-specific intrasynaptic arrangements of ionotropic glutamate receptors and their impact on postsynaptic responses. *J Neurosci* 29(41): 12896–12908.
53. Masugi-Tokita M, et al. (2007) Number and density of AMPA receptors in individual synapses in the rat cerebellum as revealed by SDS-digested freeze-fracture replica labeling. *J Neurosci* 27(8):2135–2144.
54. Harris KM, Stevens JK (1988) Dendritic spines of rat cerebellar Purkinje cells: Serial electron microscopy with reference to their biophysical characteristics. *J Neurosci* 8(12):4455–4469.
55. Palay SL, Chan-Palay V (1974) *Cerebellar Cortex: Cytology and Organization* (Springer, Berlin).
56. Sterio DC (1984) The unbiased estimation of number and sizes of arbitrary particles using the disector. *J Microsc* 134(Pt 2):127–136.
57. Lee KJ, Kim H, Kim TS, Park S-H, Rhyu IJ (2004) Morphological analysis of spine shapes of Purkinje cell dendrites in the rat cerebellum using high-voltage electron microscopy. *Neurosci Lett* 359(1–2):21–24.